Terahertz wave generation via pre-ionized air plasma

Kai Kang (康 凯)[1], Liangliang Zhang (张亮亮)[1],*, Tong Wu (吴 同)[2], Kai Li (李 凯)[3], and Cunlin Zhang (张存林)[1]

[1]*Key Laboratory of Terahertz Optoelectronics, Ministry of Education, Beijing Key Laboratory for Terahertz Spectroscopy and Imaging, and Beijing Advanced Innovation Center for Imaging Technology, Department of Physics, Capital Normal University, Beijing 100048, China*

[2]*Beijing Key Laboratory for Precision Optoelectronic Measurement Instrument and Technology, School of Optics and Photonics, Beijing Institute of Technology, Beijing 100081, China*

[3]*Daheng New Epoch Technology Inc., Beijing 100085, China*

*Corresponding author: zhlliang@126.com

We report the terahertz (THz) wave generation from a single-color scheme modulated by pre-ionized air plasma via an orthogonal pumping geometry. It is found that the amplitude of the THz signal generated by the pump beam tends to decrease gradually with the increase of the modulation power. We believe that the ponderomotive force plays an important role in the process of the interaction between the pump beam and the pre-ionization beam. The hydrostatic state of the electrostatic separation field caused by the modulation beam will directly affect the generation efficiency of the THz wave. Our results contribute to further understanding of the theoretical mechanism and expanding of the practical applications of THz wave generation and modulation.

OCIS codes: 040.2235, 350.5400, 300.6380.

doi: 10.3788/COL201816.110401.

With the research of terahertz (THz) waves, the methods of generating THz waves mainly include a photoconductive antenna[1–3], optical rectification[4,5], and laser-induced air plasma[6–8]. For the photoconductive antenna and non-linear optical crystal, the THz signal intensity increases with rise of the input energy of the pump laser and is hampered by the damage threshold of the materials. This problem has been solved since air ionization was involved in the THz wave generation process[9,10]. THz wave generation from laser-induced air plasma has been an exciting research field due to its potential applications in nondestructive examination, security imaging, ultrabroadband communication, THz nonlinear optics, and so on[11–19]. Laser-induced air plasma methods can be divided into two types: a single-color laser field that directly ionizes air to produce THz waves, which was proposed by Hamster *et al.* in 1993[20], and a two-color laser field that ionizes air to generate THz waves[21–23]. In 2011, Geints *et al.* believed that, in gases, the high-density plasma emerged because the medium photoionization prevents the beam from collapsing and light filaments are formed inside the laser beam[24].

In this Letter, we selected a single-color scheme to demonstrate the effects of pre-ionized plasma on THz wave generation via an orthogonal pumping geometry. The pre-ionization beam (modulation beam) was focused perpendicularly to the pump beam at the same point and the THz signal was detected in the direction of the pump beam. The hydrodynamic model was adopted to analyze the THz modulation effect.

The experiment setup is schematically shown in Fig. 1. The laser beam was delivered by a regenerative

p-polarized Ti:sapphire amplifier with a 50 fs pulse duration, a central wavelength of 800 nm, a 1 kHz repetition rate, and a total power of 5.2 W. The laser beam was divided by a beam splitter into two parts with the power of 1.8 W and 3.5 W respectively. The 800 nm laser with a power of 1.8 W was divided by a 94/6 beam splitter. The lower-power part was used as the probe beam, and the relative time delay between the probe and the pump beams was adjusted by a linear translation stage (not shown in the figure). The higher-power part was used as the pump beam ('Pump' in the figure), which was focused directly by a convex lens with a focal length of 150 mm to produce air plasma and generate a THz wave in the forward direction. The forward THz wave was collected, collimated, and refocused by a pair of off-axis parabolic mirrors (PMs) with a 4 inch (1 inch = 2.54 cm) equivalent focal length. The THz wave was finally focused
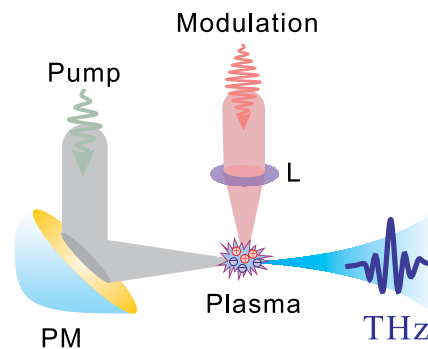
Fig. 1. Experimental setup. L: convex lens. PM: parabolic mirror.

on the ZnTe crystal collinearly with the probe beam. The mixed beam was focused by a convex lens and then detected by an auto-balanced detector. The filter was placed in the optical path between two off-axis parabolic mirrors to block the residual laser. Another part of the laser with a power of 3.5 W was used as the modulation beam ('Modulation' in the figure). In the orthogonal configuration, the modulation beam was sent through a time-delay stage and focused by a 50 mm focal length lens to create a pre-ionization air plasma crossing the plasma induced by the pump beam. The THz wave radiated from the 800 nm pre-ionization plasma was excluded from the collection of THz wave energy, since the pump beam overlapped with the pre-ionization plasma at an orthogonal angle.

We measured THz time-domain waveforms at different modulation intensities. As the modulation power ranges from 0.4 W to 1.6 W, the THz wave amplitude decreases accordingly. Figure 2(a) shows the time-domain THz waveforms at four different modulation powers ranging from 0.4 W to 1.6 W with a pump power of 0.6 W (the black line is the THz waveform without modulation). The corresponding frequency-domain spectra can be obtained by Fourier transform, as shown in Fig. 2(b).
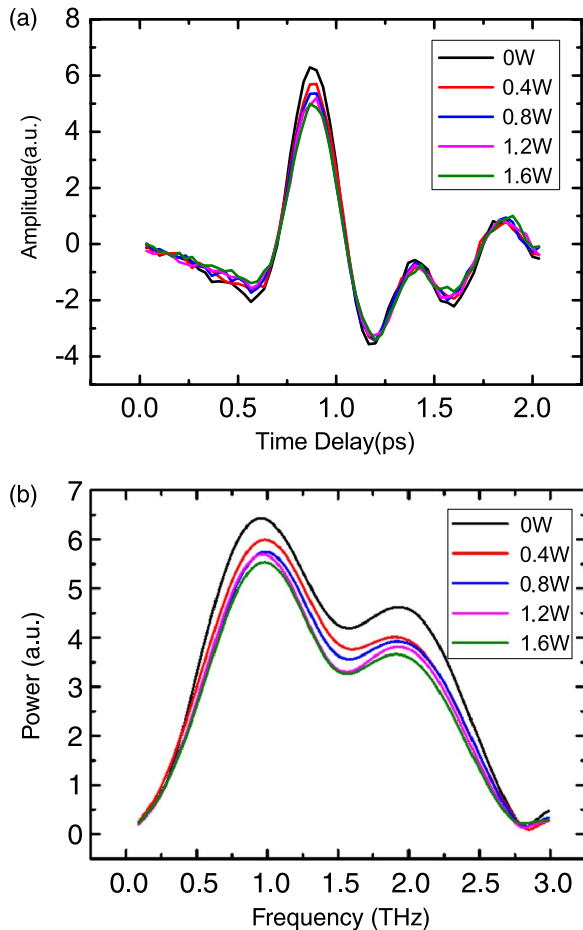
Fig. 2. (a) THz time-domain waveforms and (b) THz frequency-domain spectra with different modulation powers. The pump power is set as 0.6 W.

The THz amplitude decreases gradually with the increase of the modulation beam power. The corresponding frequency-domain amplitude also decreases and the bandwidth becomes narrower when the modulation beam power is higher.

According to the hydrodynamic model, electrons and ions are considered as two fluids. The velocities, densities, and temperatures of the two fluids satisfy the hydrodynamic equations. They are related to each other by electrostatic force and impact force, and exchange energy through collision. The Poisson equation of the electrostatic separation field ($E_{//}$) can be expressed as

$$\frac{\partial E_{//}}{\partial x} = 4\pi e(n_e u_e - Z n_i u_i). \tag{1}$$

The Helmholtz equation for the laser field ($E_\perp$) to propagate within the plasma is expressed as

$$\partial E_\perp / \partial x^2 + \kappa^2 E_\perp = 0, \tag{2}$$

where κ is the wave vector. In the above formula, subscripts e and i represent the electron and ion, respectively. n and u stand for the particle density and velocity, respectively. Particles in plasma are subjected to thermal pressure $\partial p_{e,i}/\partial x$, electrostatic forces, collision forces $\rho_i \nu_{e,i}(u_e - u_i)$, and pondermotive forces f_{NLe}, where $p_{e,i} = n_{e,i} k T_{e,i}$, k is Boltzmann's constant and $T_{e,i}$ is temperature, and ρ represents the mass density. The pondermotive force of particles can be expressed as

$$f_{NLe} = \frac{q^2}{4m\omega}\Delta E^2(x), \tag{3}$$

where ω is the angular frequency of the laser and E is the amplitude of the laser field. With the effect of E, the electron has scattered out in the direction perpendicular to the optical path and experienced the process of accelerating and decelerating in the direction of the optical path. Due to the great difference in the mass of ions and electrons, the pondermotive force received is also greatly different, which results in a strong electrostatic separation field. Then the electrons and ions speed up or decelerate in the transient electric field to form a transient current. In this model, another strong force is thermal pressure, which is caused by electrons. Absorbing the laser energy efficiently, the electron temperature rises rapidly, and produces strong thermal pressure on the two sides of the low-temperature region, pushing the electrons to move quickly to both sides. So neutrality is destroyed again and another electrostatic separation field has been created that drives the movement of ions and electrons to the regions with low electron temperatures, resulting in a powerful electromagnetic transient and eventual THz wave generation.

When the two laser beams are vertically focused at one point on the same horizontal plane, we believe that the plasma is nearly orthogonal in space to form a more complex plasma region. In this area, the pre-ionization plasma plunders parts of electrons and ions and these particles

become meaningless for the generation of a THz wave. For this reason, ρ, n, and u decrease so that the electric field amplitude (E) and the particle motion velocity, as well as the acceleration, directly reduce under the influence of the pondermotive force and the thermal pressure, which leads to the reduction of the THz wave intensity.

In our experiments, we also calculated the dependence of THz wave energy on the arrival time of the pre-ionization plasma generation pulse with respect to the pump beam. The integral over the square of the whole THz waveform gives the energy of the THz pulse. The intensity of THz radiation varies sharply with the intersection of two plasmas in the spatial and temporal domains. First, we optimize the experimental system to make the two plasmas orthogonal in space. Then a translator is placed in the modulation path to adjust the time delay. When the two beams are consistent in the time and space domains, modulation occurs, as shown in Fig. 3(a). In the early stage (0–5 ps), the pump beam arrives at the cross region prior to modulation; when adjusting the translation platform, the two beams arrive at the cross region together at 5 ps and the duration of the modulation process is 3 ps. After 8 ps, the modulation breaks away from the cross region, and the peak value begins to recover slowly. For clarity, the curves corresponding to the three representative pump beam powers of 0.4 W, 0.6 W, and 0.8 W to generate THz waves are shown.

Here, we define a THz wave modulation depth $M = (S_1 - S_2)/S_1$ to predict the degree of the pre-ionization suppression on the THz wave intensity, where S_1 is the THz wave signal generated by the pump beam without pre-ionization plasma, and S_2 is the THz wave signal when the 800 nm pre-ionization plasma is prior to the arrival of the pump beam[25]. Figure 3(b) shows the effect of the modulated laser intensity on the THz wave modulation depth. There are two orthogonal pondermotive force fields in the cross region, and changing the power of any beam will affect the THz radiation. First, when the pump beam power is constant, the stronger the modulated beam is, the more electrons become useless for THz wave generation. The weaker the intensity of the THz wave, the stronger the modulation depth. Second, when the modulation power remains constant, the stronger the pump beam power is, the more electrons become useful for THz wave generation. What is more, the greater the intensity of the THz wave, the lower the modulation depth. However, when the modulation power is less than 0.6 W, the result somewhat deviates from our theory. We believe that it is the low modulation power and the error caused by the experimental measurement that result in the indistinct discrimination.

Figure 4 shows the THz wave polarization under different modulation powers with a fixed pump power of 0.8 W. It is obvious that the THz wave polarization stays linear and its direction does not rotate with the increase of the modulation power. The results are basically consistent with the expectations of our analysis. The effect of the lateral modulation beam reduces the excitation of the
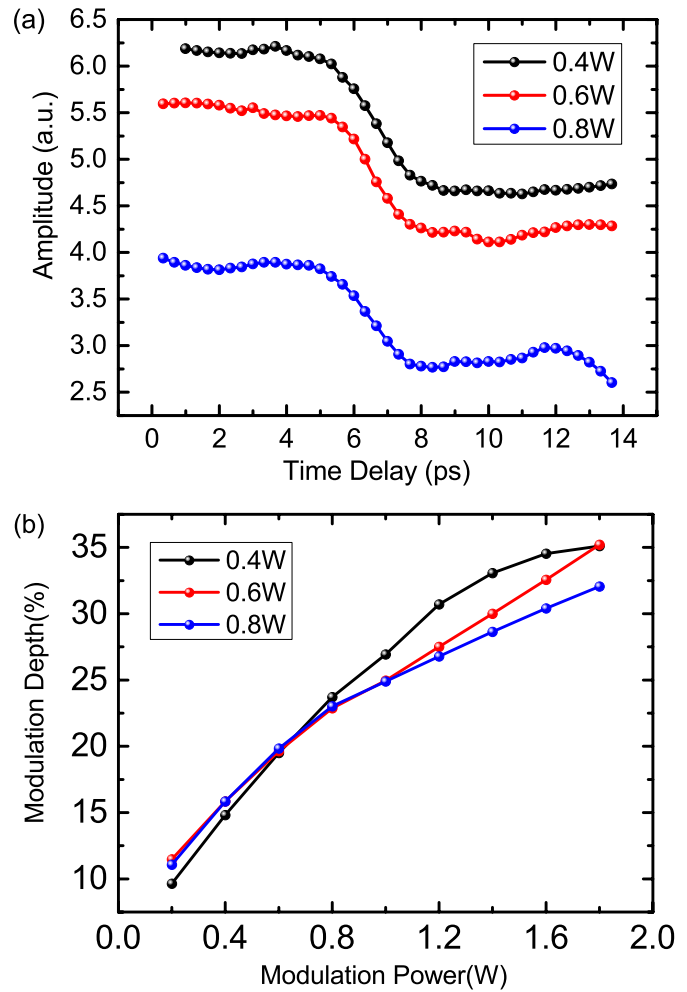
Fig. 3. (a) THz signal of three representative excitation pump powers of 0.4 W, 0.6 W, and 0.8 W in the presence of pre-formed plasma as a function of the relative time between the pump beam and the modulation beam. (b) The effect of the modulated laser intensity on the THz wave modulation depth.

longitudinal pump beam, so that some particles do not participate in the THz wave generation. It does not substantially change the general structure of the plasma, so it does not change the THz polarization.

In conclusion, we demonstrated that the THz wave energy modulation depth depends upon the energy of the pump pulse when a pre-ionization plasma is created by a synchronized modulation beam using an orthogonal pumping geometry. We found that the THz wave modulation depth increases as a function of the modulation beam power. When the power of the modulation beam increases, the THz wave modulation tends to be saturated. Our results contribute to further understanding of the theoretical mechanism and expanding of the practical applications of THz wave generation and modulation.
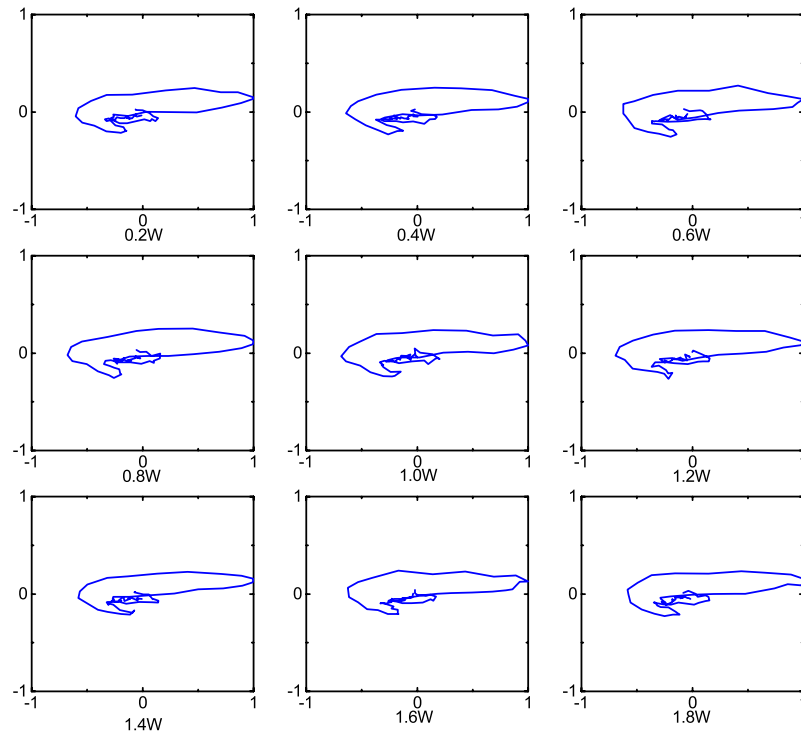
Fig. 4. THz wave polarization under different modulation powers.

References

1. D. H. Auston, K. P. Cheung, and P. R. Smith, Appl. Phys. Lett. **45**, 284 (1984).
2. J. T. Darrow, B. B. Hu, X. C. Zhang, and D. H. Auston, Opt. Lett. **15**, 323 (1990).
3. N. M. Froberg, B. B. Hu, X. C. Zhang, and D. H. Auston, Appl. Phys. Lett. **59**, 3207 (1991).
4. A. Rice, Y. Jin, X. F. Ma, X. C. Zhang, D. Bliss, and J. Larkin, Appl. Phys. Lett. **64**, 1324 (1994).
5. X. Xie, J. Dai, and X. C. Zhang, Phys. Rev. Lett. **96**, 075005 (2006).
6. A. Mysyrowicz, B. Prade, G. Beaudin, G. Méchain, G. Patalano, and J. M. Munier, Opt. Lett. **27**, 1944 (2002).
7. J. Dai and X. C. Zhang, Appl. Phys. Lett. **94**, 1210 (2009).
8. H. W. Du, H. Hoshina, C. Otani, and K. Midorikawa, Appl. Phys. Lett. **107**, 2725 (2015).
9. M. Kress, T. Löffler, S. Eden, M. Thomson, and H. G. Roskos, Opt. Lett. **29**, 1120 (2004).
10. T. Löffler, M. Kress, M. Thomson, and H. G. Roskos, Acta Phys. Pol. **107**, 99 (2005).
11. N. Karpowicz, J. Dai, X. Lu, Y. Chen, M. Yamaguchi, and H. Zhao, Appl. Phys. Lett. **92**, 1759 (2008).
12. M. Clerici, M. Peccianti, B. E. Schmidt, L. Caspani, M. Shalaby, and A. Lotti, Phys. Rev. Lett. **110**, 253901 (2013).
13. K. Y. Kim, A. J. Taylor, J. H. Glownia, and G. Rodriguez, Nat. Photon. **2**, 605 (2008).
14. X. Y. Peng, C. Li, M. Chen, T. Toncian, R. Jung, and O. Willi, Appl. Phys. Lett. **94**, 1120 (2009).
15. M. D. Thomson, V. Blank, and H. G. Roskos, Opt. Express **18**, 23173 (2010).
16. T. I. Oh, Y. S. You, N. Jhajj, and E. W. Rosenthal, Appl. Phys. Lett. **102**, 1210 (2013).
17. Y. Minami, T. Kurihara, K. Yamaguchi, M. Nakajima, and T. Suemoto, Appl. Phys. Lett. **102**, 041105 (2013).
18. J. Shin, Z. Jin, T. Hosokai, and R. Kodama, in *Asia Pacific Physics Conference* (2013).
19. J. Zhao, L. Zhang, Y. Luo, T. Wu, C. Zhang, and Y. Zhao, Chin. Opt. Lett. **12**, 083201 (2014).
20. H. Hamster, A. Sullivan, S. Gordon, W. White, and R. W. Falcone, Phys. Rev. Lett. **71**, 2725 (1993).
21. Y. Bai, J. Tang, R. Xu, and P. Liu, Chin. Opt. Lett. **14**, 093201 (2016).
22. W. Wang, Z. Sheng, Y. Li, L. Chen, Q. Dong, X. Lu, J. Ma, and J. Zhang, Chin. Opt. Lett. **9**, 110002 (2011).
23. Q. Wang, Y. Zhang, Z. Wang, J. Ding, Z. Liu, and B. Hu, Chin. Opt. Lett. **14**, 110201 (2016).
24. Y. E. Geints, A. M. Kabanov, A. A. Zemlyanov, E. E. Bykova, O. A. Bukin, and S. S. Golik, Appl. Phys. Lett. **99**, 181114 (2011).
25. T. Wu, L. Dong, S. Huang, R. Zhang, S. Zhang, and H. Zhao, Appl. Phys. Lett. **112**, 171106 (2018).